

PCCP

Accepted Manuscript



This is an *Accepted Manuscript*, which has been through the Royal Society of Chemistry peer review process and has been accepted for publication.

Accepted Manuscripts are published online shortly after acceptance, before technical editing, formatting and proof reading. Using this free service, authors can make their results available to the community, in citable form, before we publish the edited article. We will replace this *Accepted Manuscript* with the edited and formatted *Advance Article* as soon as it is available.

You can find more information about *Accepted Manuscripts* in the [Information for Authors](#).

Please note that technical editing may introduce minor changes to the text and/or graphics, which may alter content. The journal's standard [Terms & Conditions](#) and the [Ethical guidelines](#) still apply. In no event shall the Royal Society of Chemistry be held responsible for any errors or omissions in this *Accepted Manuscript* or any consequences arising from the use of any information it contains.

Cite this: DOI: 10.1039/c0xx00000x

www.rsc.org/xxxxxx

Nonidentical Intracellular Drug Release Rates in Raman and Fluorescence Spectroscopic Determination

Erdene-Ochir Ganbold,^a Jinha Yoon,^a Doseok Kim,^b and Sang-Woo Joo^{*,a}

Acceptance Data [DO NOT ALTER/DELETE THIS TEXT]

Publication data [DO NOT ALTER/DELETE THIS TEXT]

DOI: 10.1039/b000000x [DO NOT ALTER/DELETE THIS TEXT]

Intracellular drug release rates were measured by monitoring mitoxantrone (MTX) on gold nanoparticle (AuNP) carriers by means of real-time label-free bimodal imaging with confocal Raman and fluorescence spectroscopy. The quenching nature of the MTX-AuNPs by nanometal surface energy transfer (NSET) was analyzed with the determined Stern–Volmer constant of $K_{SV} = 2.28 \times 10^9 \text{ M}^{-1}$. The amount of MTX released was estimated by both the decrease in the surface-enhanced resonance Raman scattering (SERRS) signal and the increase in the fluorescence intensity. Both SERRS and NSET provide quantitative relationships between the spectral intensities of MTX concentrations in solution. Inside live cells, the signal decay profiles of the drug release from AuNPs appeared to be faster at the beginning of the bond-breaking drug release for the SERRS (R^{-12}) than the recovery time of the NSET (R^{-4} or R^{-6}). In the first 45 min, a rather fast decay rate k of 0.0252 min^{-1} with a short half-life $t_{1/2}$ of 27.5 min was observed, whereas the rate became significantly slower in a diffusion process, 0.0093 min^{-1} with a longer half-life of 101.4 min, after 45 min.

Surface-enhanced Raman scattering (SERS) has recently attracted much attention to materials chemistry.¹ Although SERS has been utilized for biological sensing and molecular imaging,² the selection rules imposed by electromagnetic effects and charge transfer have made its analytical use problematic.³ On the other hand, quantitative surface-enhanced resonance Raman scattering (SERRS) studies have been utilized to ratiometrically analyze biological samples.⁴ Distance dependence^{5–7} in the SERS were reportedly determined in the range from R^{-10} to R^{-12} .

In nano- and biotechnology, particular attention has been paid to the monitoring of the amount of drugs in drug delivery systems (DDSs) followed by the release to intracellular compartments in vitro and in vivo.⁸ In regard to nanoparticle-based DDSs, the development of diverse sensing methods has been challenging because of instrumental limitations of the various spectroscopic tools that have been used so far. Gold nanoparticle (AuNP)-based drug delivery systems have long been investigated as efficient tools for chemotherapeutics because of their low toxicity and biocompatibility.⁹

Organic fluorophores used as a signal source suffer from frequent problems such as background noise, autofluorescence, tissue scattering, and photobleaching.¹⁰ The additional disadvantages of optical methods include interference from surrounding media and a low spatial resolution.¹¹ Raman

microscopy is one possible way of overcoming the drawbacks of fluorescence spectroscopy, and this method has recently made distinctive contributions to intracellular monitoring.¹²

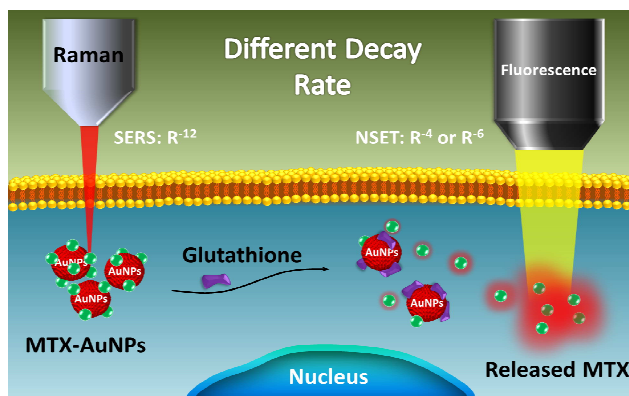


Fig. 1 Observation of different intracellular decay rates via bimodal imaging technology using SERS and NSET.

The fluorescence of certain molecules on metal nanoparticle surfaces can be quenched through nanometal surface energy transfer (NSET).¹³ The fluorescence quenching efficiency of AuNPs has been reported to be 10^7 – 10^{11} M^{-1} based on a calculation using the Stern–Volmer equation.¹⁴ NSET has a longer distance dependency of either R^{-4} or R^{-6} in the Chance–Prock–Silbey (CPS)–Kuhn¹⁵ and Gerstein–Nitzan (G–N) models,¹⁶ respectively. On the other hand, because of the electromagnetic effect and selection rules^{17–19} of SERS, the enhancement may be proportional to the electric field as $|E|^4$, where E decays as R^{-3} . Thus, it is anticipated that the SERS

^a Erdene-Ochir Ganbold, Jinha Yoon, and Prof. Sang-Woo Joo, Department of Soongsil University, Seoul 156-743 Korea, E-mail: sjoo@ssu.ac.kr.ac.kr

^b Prof. Doseok Kim, Department of Physics, Sogang University, Seoul 121-742, Korea

† Electronic Supplementary Information (ESI) available: See DOI: 10.1039/b000000x/

intensity decreases with distance as R^{-12} , and it is expected that SERS would be more rapidly influenced by the distance in the proximate region on AuNP surfaces because of the longer-distance dependency of the NSET-induced fluorescence quenching of R^{-4} or R^{-6} . This would, importantly, result in different decay rates in the drug release from AuNPs for SERS and fluorescence quenching and may provide a unique intracellular optical-based molecular ruler.

Previous *in vitro* and *in vivo* SERS studies required the employment of Raman reporter tags such as malachite green isothiocyanate (MGI) and crystal violet (CV).²⁰ The label-free SERS method we implement in this study, however, does not need additional organic dye molecules, as it provides direct information about surface reactions.²¹ Despite the versatile spectral features of Raman spectroscopy, bimodal imaging with the aid of other independent spectroscopic techniques may be a prerequisite owing to the equivocal selection rules and problematic quantification of SERS intensities.²²

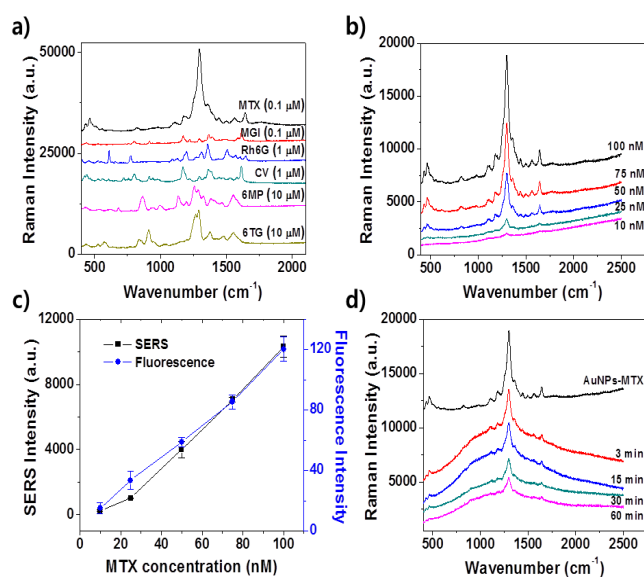


Fig. 2 (a) Comparative SERS spectra of MTX (0.1 μM) with MGI (0.1 μM), Rh6G (1 μM), CV (1 μM), 6MP (10 μM), and 6TG (10 μM). (b) Concentration-dependent SERS spectra of MTX between 10–100 nM. (c) Quantitative aspects of SERS and fluorescence intensities as a function of the MTX concentration. Peaks at 1291 cm^{-1} were used to compare the relative intensities. Error bars demonstrate the standard deviation of three measurements. (d) GSH concentration-dependent SERS intensities of MTX (100 nM) on AuNP surfaces in an aqueous solution, exhibiting the background changes due to the increase in fluorescence.

Mitoxantrone (MTX), an anticancer drug adsorbed on metal nanoparticles, is known to exhibit extremely strong SERS signals along with strong fluorescence.^{23,24} In this study, by using MTX-AuNP complexes, we could measure the drug release rate by SERS as well as qualitatively identify the drug release to cancer cells by fluorescence spectroscopy. Fig. 1 demonstrates graphically an overview of our investigations in this study. The detached MTX drug can be monitored by both a SERS signal decrease and a fluorescence intensity increase upon irradiation. The signal decay profiles of the drug release from AuNPs appeared to be dissimilar for fluorescence quenching with SERS and NSET. To the best of our knowledge, the determination including the discussion of different intracellular drug release rates by bimodal imaging technology using SERS and NSET for DDSs has not been reported.

MTX on AuNPs appeared to exhibit strong Raman intensities upon excitation at 633 nm through a resonance-enhancement process, showing the spectra of MTX and AuNPs, as depicted in Figs. S1. These SERS spectra are consistent with the findings in previous reports.^{23,24} The enhancement factor was estimated to be as high as 2.5×10^6 under our experimental conditions. Moreover, the SERS intensities of MTX were observed to be larger than those of thiopurine anticancer drugs^{25,26} such as 6-mercaptopurine (6MP) and 6-thioguanine (6TG) by a factor of greater than 100. In addition, the SERS intensities of MTX appeared to be stronger than those of conventional dyes such as rhodamine 6G (Rh6G), crystal violet (CV), and malachite green isothiocyanate (MGI), as shown in Fig. 2a. Fig. 2c shows the calibration curves of both the SERS and fluorescence intensities as a function of the MTX concentration. Fig. 2d and Fig. S2 show GSH concentration-dependent SERS intensities of MTX.

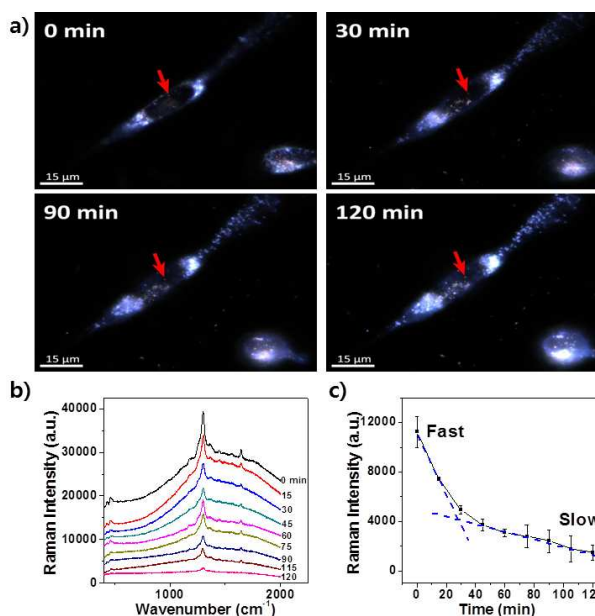


Fig. 3 (a) Photographs of the time-dependent *in vitro* dark-field microscopy (DFM) of live cell images. The arrows indicate the location of the AuNPs according to the SERS spectra. (b) Time-dependent SERS spectra of MTX-conjugated AuNPs exhibiting the release of MTX. (c) Intensity of the SERS spectra of MTX-AuNPs determined by measuring the intensities of the MTX peak at 1291 cm^{-1} . The standard deviations were obtained from independent measurements of three different cells.

Fig. 3 shows the *in vitro* release of MTX from AuNPs in HeLa cells over a time interval of 0–120 min. We observed the AuNPs inside the cell membrane using a z-dependent SERS method (see Fig. S3a, ESI†). Raman monitoring implies that the SERS intensities of MTX were decreased inside the cells in an hour. The decay profiles could be divided into two distinct regions as shown in Fig. 3c. In the first 45 min, a rather fast decay rate k of 0.0252 min^{-1} with a short half-life $t_{1/2}$ of 27.5 min was observed, whereas the rate became significantly slower, 0.0093 min^{-1} with a longer half-life of 101.4 min, after 45 min. The initial fast decay may be due to a bond breaking process between MTX and the AuNPs. The subsequent slower rate may be interpreted as the non-quantitative nature of the SERS intensity such as hot spots, where only a few percent of the adsorbates can yield a majority of the total intensity.

1×10^5 HeLa cells were seeded on 35×50 mm gelatin-coated cover glass and incubated at 37°C in 5% CO_2 atmosphere for 24 h. After treating with MTX-conjugated AuNPs, the cells were incubated for another 24 h. A cell-attached cover glass was reversely placed in the live cell chamber as shown in the above scheme. The live cell chamber is connected to the culture medium containing a syringe by a flexible tube. We performed Raman measurements along the z-axis to identify whether AuNPs are inside the cell. Internalized AuNPs are recognized from the intracellular organelles by characteristic vibrational bands of the drug molecules as well as their yellowish color.

It is difficult to say whether the number of AuNPs where we record Raman spectra decreases or increases. Although maintaining the same number of AuNPs using our experimental setup is impossible, in most cases, no significant change in the size of the accumulated AuNPs was observed by microscopic images and the naked eye through an objective lens during the measurements.

AuNPs in the microscopic images do not enter the nucleus but are accumulated in the cytosol.²⁷ AuNPs located between the outer cell membrane and the nucleus may appear as if they are inside the nucleus when microscopic images are taken using the objective lens.

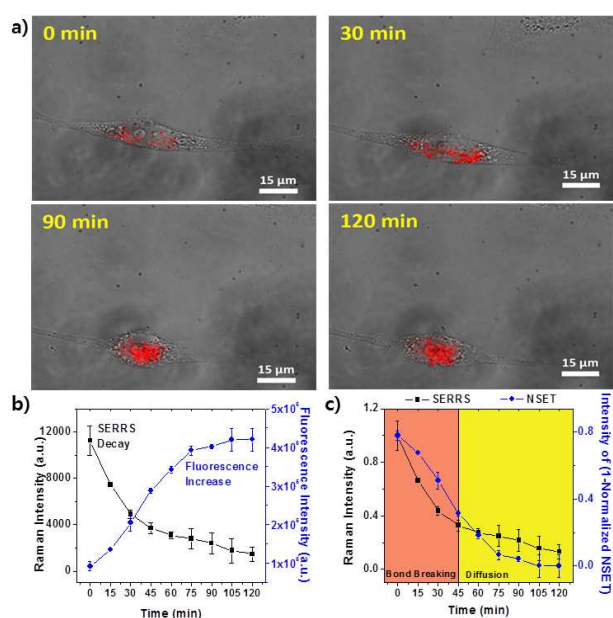


Fig. 4 (a) In vitro fluorescent images of live cells exhibiting the release of MTX from AuNPs. (b) Combined intensity plot of the MTX fluorescence spectra and MTX-conjugated AuNPs SERS spectra. (c) Comparative calibration curves of SERRS and NSET (1-normalized fluorescent intensities with respect to the maximum value) in a single cell. Note that the initial rapid and subsequent slow decay regions can correspond to a bond breaking stage and a diffusion process, respectively.

As in a previous report,³ the hottest sites amount to just 63 in a total of 1,000,000, but they contribute 24% of the overall SERS intensity. Considering that the SERRS intensities did not completely disappear despite the GSH replacement as indicated in Fig. 3d, a very small amount of MTX on AuNPs may yield strong SERRS intensities.

Based on these Raman data, we performed an independent fluorescent live-cell imaging experiment under the same

experimental conditions. The fluorescence spectra exhibited a quantitative behavior in the MTX concentration range of 10 nM to 1.0 μM (see Fig. S1b, ESI[†]). The quenching nature of the MTX–AuNP system with AuNP concentrations of 100–500 pM can be analyzed by the Stern–Volmer equation¹⁴ with a determined constant of $K_{SV} = 2.28 \times 10^9 \text{ M}^{-1}$ (see Fig. S1c, ESI[†]). This result supports the idea that the quenched fluorescence may be recovered when MTX desorbs on AuNPs. Fig. 4a demonstrates that the MTX-assembled AuNPs were well internalized into mammalian cancer cells, and most of the MTX (40 nM) attached to the AuNPs was released within an hour, as indicated in Figs. 4b and 4c. Less rapid attenuation of the signal intensities was observed for the fluorescence data than for the SERRS spectral data. SERRS appeared to be more influenced by the distance in the proximate region on the AuNP surfaces because of the rather longer-distance dependency of the metal-induced fluorescence quenching $(R + R_0)^{-4}$ compared to that of SERS $[1/1 + (R/a_0)]^{12}$.

In the initial stage between 0–45 min, we could observe more rapid decrease in the SERRS measurement and a lag time in the NSET decay. This can be ascribed to a bond-breaking process that MTX would start to detach from AuNPs, if the difference in their distance dependence of the two methods is taken into account. The next decay profile between 45–120 min may be regarded as a typical diffusion-controlled process that can be fitted as a power law of $m > 0.5$ in the equation of $C/C_0 = Kt^m$, where C and C_0 are the concentrations at the given times of t and zero, respectively.²⁸ The detached MTX spread out inside the cellular medium via either Fickian diffusion or non-Fickian relaxation/transport processes. Considering that the molecular weight and its estimated diffusion coefficient D value of 10^{-5} – $10^{-4} \text{ cm}^2/\text{sec}$ for MTX,²⁹ the diffusion length were estimated to be much longer than those of the dimension of AuNP aggregates inside either endosome or lysosome, which would be as short as 1 μm. (see Fig. S4, ESI[†]).

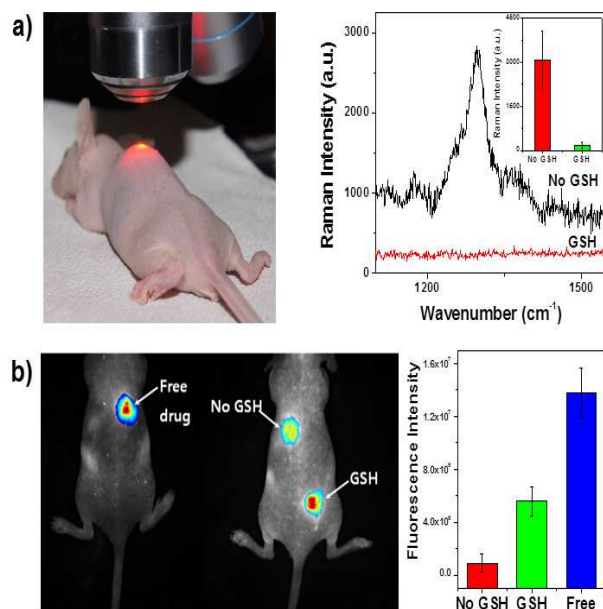


Fig. 5 (a) Photograph of the in vivo resonance Raman monitoring of GSH-triggered release (left). PEGylation was introduced to obtain the Raman peaks. In vivo SERRS spectra of MTX and MTX–AuNPs in the presence and absence of GSH (right). The MTX peak at $1,291 \text{ cm}^{-1}$ almost disappeared after applying GSH. (b) In vivo fluorescence images of mice (left). Bar graph of the fluorescence intensities (right).

A rather slow decay curve between 45–120 min may be due to an encapsulated state of MTX-AuNPs, which can affect and retard the diffusion process of free MTX. After 90 min, the NSET intensity became almost unchanged, which indicated that most MTX became alienated from AuNPs. In contrast to the NSET intensities, the significant SERRS intensities after a prolonged time of 60–120 min may be due to a trace amount of MTX on AuNPs in hot spots, which yields the signal in a non-quantitative way even on the decreased surface coverage density. Thus, fluorescent live-cell imaging techniques in comparison with SERRS yielded different decay rates in the estimation of drug release. Based on the average diameter of the AuNPs and a previous report on the value of R_o ,³⁰ the distances for which the SERS and NSET would decrease by 50% would be 0.46 and 22 nm, respectively, assuming similar quenching behavior of MTX and cyanine-3B ($\lambda_{\text{max}} = 570$ nm) for ~15-nm AuNPs. It has to be mentioned that both a single cell microscopic and numerous cell ($>10^3$) fluorescence measurements using a microreader exhibited the similar decay profiles (see Fig. S5c, ESI†).

In vivo images indicated that MTX release could be estimated by both Raman and fluorescence microscopy as shown in Fig. 5. As GSH was injected into the tumor site where the MTX-assembled AuNPs were previously applied, the SERS signals almost disappeared, whereas the fluorescence intensities increased substantially.

Our work envisages that bimodal spectroscopic determination using Raman and fluorescence spectroscopy will be useful for monitoring the delivery kinetics of drug molecules from AuNPs inside cancer cells in DDS development.

Prof. D. Kim acknowledges support from the Korea government (MEST) No. 2011-0031496. SWJ would like to thank Jaemin Lee, Dr. Dheeraj Singh, Prof. Jong Seung Kim, Prof. Kwang-Hie Cho, Prof. So Yeong Lee, and Prof. Jaebum Choo for their kind help in preparing the manuscript.

Notes and references

- (a) G. W. Lu, C. Li and G. Q. Shi, *Chem. Mater.*, 2007, **19**, 3433–3440; (b) L. Chen, Y. Gao, H. Xu, Z. Wang, Z. Li and R-Q. Zhang, *Phys. Chem. Chem. Phys.*, 2014, **16**, 20665–20671; (c) W.-H. Park and Z. H. Kim, *Nano Lett.* 2010, **10**, 4040–4048; (d) T. Ghosh, P. Das, T. K. Chini, T. Ghosh and B. Satpati, *Phys. Chem. Chem. Phys.*, 2014, **16**, 16730–16739.
- S. Ayas, G. Cinar, A. D. Ozkan, Z. Soran, O. Ekiz, D. Kocaay, A. Tomak, P. Toren, Y. Kaya, I. Tunc, H. Zareie, T. Tekinay, A. B. Tekinay, M. O. Guler and A. Dana, *Sci. Rep.*, 2013, **3**, 2624.
- Y. Fang, N. H. Seong and D. D. Dlott, *Science*, 2008, **321**, 388–392.
- A. Pallaoro, G. B. Braun and M. Moskovits, *Proc. Natl. Acad. Sci. U S A*, 2011, **108**, 16559–16564.
- B. J. Kennedy, S. Spaeth, M. Dickey and K. T. Carron, *J. Phys. Chem. B*, 1999, **103**, 3640–3646.
- G. Compagnini, C. Galati and S. Pignataro, *Phys. Chem. Chem. Phys.*, 1999, **1**, 2351–2353.
- K. Kneipp, H. Kneipp, I. Itzkan, R. R. Dasari and M. S. Feld, *J. Phys. Condens. Matter*, 2002, **14**, R597–R624.
- M. Fretz, J. Jin, R. Conibere, N. A. Penning, S. Al-Taei, G. Storm, S. Futaki, T. Takeuchi, I. Nakase and A. T. Jones, *J. Control Release*, 2006, **116**, 247–254.
- A. M. Alkilany, S. E. Lohse and C. J. Murphy, *Acc. Chem. Res.*, 2013, **46**, 650–661.
- S. Bencic-Nagale and D. R. Walt, *Anal. Chem.* 2005, **77**, 6155–6162.
- X. Cai, W. Li, C-H. Kim, Y. Yuan, L. V. Wang, Y. Xia, *ACS Nano*, 2011, **5**, 9658–9667.

- H. Xu, Q. Li, L. Wang, Y. He, J. Shi, B. Tang and C. Fan, *Chem. Soc. Rev.*, 2014, **43**, 2650–2661.
- T. Sen, K. K. Haldar and A. Patra, *J. Phys. Chem. C*, 2008, **112**, 17945–17951.
- U. H. Bunz and V. M. Rotello, *Angew. Chem. Int. Ed.*, 2010, **49**, 3268–3279.
- R. R. Chance, A. Prock and R. Silbey, *J. Chem. Phys.*, 1975, **62**, 2245–2253.
- J. Gersten and A. Nitzan, *J. Chem. Phys.*, 1981, **75**, 1139–1152.
- M. Moskovits, *Rev. Mod. Phys.*, 1985, **57**, 783–826.
- E. C. Le Ru M. Meyer, E. Blackie and P. G. Etchegoin, *J. Raman Spectrosc.*, 2008, **39**, 1127–1134.
- A. Creighton, *Surf. Sci.*, 1983, **124**, 209–219.
- X. Qian, X. H. Peng, D. O. Ansari, Q. Yin-Goen, G. Z. Chen, D. M. Shin, L. Yang, A. N. Young, M. D. Wang and S. Nie, *Nat. Biotechnol.*, 2008, **26**, 83–90.
- S. M. Asiala and Z. D. Schultz, *Anal. Chem.*, 2014, **86**, 2625–2632
- A. M. Gabudean, D. Biro and S. Astilean, *Nanotechnology*, 2012, **23**, 485706.
- I. Nabiev, A. Baranov, I. Chourpa, A. Beljebbar, G. D. Sockalingum and M. Manfait, *J. Phys. Chem.*, 1995, **99**, 1608–1613.
- G. Breuzard, O. Piot, J. F. Angiboust, M. Manfait, L. Candeil, M. del Rio and J. M. Millot, *Biochem. Biophys. Res. Commun.*, 2005, **329**, 64–70.
- K. Ock, W. I. Jeon, E. O. Ganbold, M. Kim, J. Park, J. H. Seo, K. Cho, S. W. Joo and S. Y. Lee, *Anal. Chem.*, 2012, **84**, 2172–2178.
- M. Kim, K. Ock, K. Cho, S. W. Joo and S. Y. Lee, *Chem. Commun.*, 2012, **48**, 4205–4207.
- B. D. Chithrani, A. A. Ghazani and W. C. W. Chan, *Nano Lett.*, 2006, **6**, 662–668.
- J. Siepmann and N. A. Peppas, *Adv. Drug Deliver. Rev.*, 2001, **48**, 139–157.
- M. Enache, I. Anghelache and E. Volanschi, *Int. J. Pharm.*, 2010, **390**, 100–106.
- C. J. Breshike, R. A. Riskowski and G. F. Strouse, *J. Phys. Chem. C*, 2013, **117**, 23942–23949.